Synthesis, structure, and electrical behavior of $Sr_4Bi_4Ti_7O_{24}$

M. A. Zurbuchen, V. O. Sherman, A. K. Tagantsev, J. Schubert, M. E. Hawley, D. D. Fong, S. K. Streiffer, Y. Jia, W. Tian, and D. G. Schlom

Citation: Journal of Applied Physics **107**, 024106 (2010);
View online: https://doi.org/10.1063/1.3273388
View Table of Contents: http://aip.scitation.org/toc/jap/107/2
Published by the American Institute of Physics

Synthesis, structure, and electrical behavior of $Sr_4Bi_4Ti_7O_{24}$

M. A. Zurbuchen,[1,a)] V. O. Sherman,[2] A. K. Tagantsev,[2] J. Schubert,[3] M. E. Hawley,[4] D. D. Fong,[5] S. K. Streiffer,[6] Y. Jia,[7] W. Tian,[7] and D. G. Schlom[7]
[1]*Microelectronics Technology Department, The Aerospace Corporation, El Segundo, California 90245, USA*
[2]*Laboratorie de ceramique, École Polytechnique Fédérale de Lausanne, CH-1015 Lausanne, Switzerland*
[3]*IBN1-IT and JARA-Fundamentals of Future Information Technologies, Forschungszentrum Jülich GmbH, 52425 Jülich, Germany*
[4]*Materials Science and Technology Division, Los Alamos National Laboratory, Los Alamos, New Mexico 87545, USA*
[5]*Materials Science Division, Argonne National Laboratory, Argonne, Illinois 60439, USA*
[6]*Center for Nanoscale Materials, Argonne National Laboratory, Argonne, Illinois 60439, USA*
[7]*Department of Materials Science and Engineering, Cornell University, Ithaca, New York 14853, USA*

(Received 23 July 2009; accepted 17 November 2009; published online 25 January 2010)

An $n=7$ Aurivillius phase, $Sr_4Bi_4Ti_7O_{24}$, with $c=6.44$ nm, was synthesized as an epitaxial (001)-oriented film. This phase and its purity were confirmed by x-ray diffraction and transmission electron microscopy. The material is ferroelectric, with a $P_r=5.3\ \mu C/cm^2$ oriented in the (001) plane and a paraelectric-to-ferroelectric transition temperature of $T_C=324$ K. Some indications of relaxorlike behavior are observed. Such behavior is out of character for $Sr_{n-1}Bi_2Ti_nO_{3n+3}$ Aurivillius phases and is closer to the bulk behavior of doped $SrTiO_3$, implying a spatial limit to the elastic interlayer interactions in these layered oxides. A finite-element solution to the interpretation of data from interdigitated capacitors on thin films is also described. © *2010 American Institute of Physics*. [doi:10.1063/1.3273388]

I. INTRODUCTION

Many recent discoveries of striking electromagnetic material phenomena have been made in layered perovskite oxides, including colossal magnetoresistance,[1] nearly fatigue-free ferroelectricity,[2] natural multiferroic nanocomposites,[3] thermoelectricity,[4] and high-T_C superconductivity,[5] enabling new devices such as nonvolatile computer memories. Layered perovskite oxides also serve as model material systems for the study of diminishing interactions between structural layers and as pseudo-two-dimensional systems.[6,7] The seemingly inexhaustible variety of layering schema provides a wealth of complex behaviors that will doubtless provide many more surprising discoveries.

Unfortunately, experimental access to a great number of layered oxides is blocked by thermodynamics, especially to those with large layering periods. The difference in formation enthalpy between different layering orders of similar composition is too subtle to stabilize one phase relative to others, at least by conventional solid state methods.[8–41]

The result is a diminishingly small thermodynamic driving force for formation of any individual phase, resulting in a high degree of intergrowths in bulk-processed samples. Indeed, if the enthalpy of a single n phase and a mixture of different-n intergrowths are sufficiently equivalent, the free energy of formation for the mixture will be lower, due to its greater configurational entropy.[42]

Some success in overcoming this barrier has been reported for synthesis of layered oxide films via sequential physical deposition techniques (e.g., molecular-beam epitaxy), in which both layer charge and the intermittent delivery of adatoms of high sticking coefficient are used to control phase formation.[43–47] This approach is generally not feasible for the synthesis of Aurivillius phases (defined below), however, due to the nonzero electronic charge of individual atomic layers. Success has been reported for $Bi_4Ti_3O_{12}$, which crystallizes in charge-neutral formula units,[43] but success via this route with larger unit-celled materials remains elusive.

The disparity in the charge of atomic layers can be exploited with epitaxial codeposition growth techniques, such as pulsed laser deposition (PLD), to yield layer ordering mediated by this charge. Compositions can be chosen to exploit the natural tendency to minimize electronic surface-charge and to impose a particular layer order *during growth* of a thin film, to force the crystallization of material to occur in a particular order by tailoring composition to result in large electronically neutral structural units. This breakthrough in the formulation and charge-mediated synthesis of layered oxides enables the growth of new phases having much larger periods than previously achieved by any synthesis technique.

In this paper, we describe the synthesis of a very-large-period layered oxide of the Aurivillius type, $Sr_4Bi_4Ti_7O_{24}$. The phase purity, microstructure, and electronic polarization behavior along multiple axes are reported. An analytical solution for the capacitance of interdigitated capacitors (IDCs) is also reported as used to derive the dielectric constant and remanent polarization of the material. The solution provides a means for interpreting electrical measurement results for ferroelectric films having similar geometry and thickness.

[a)]Author to whom correspondence should be addressed. Electronic mail: mark.a.zurbuchen@aero.org.

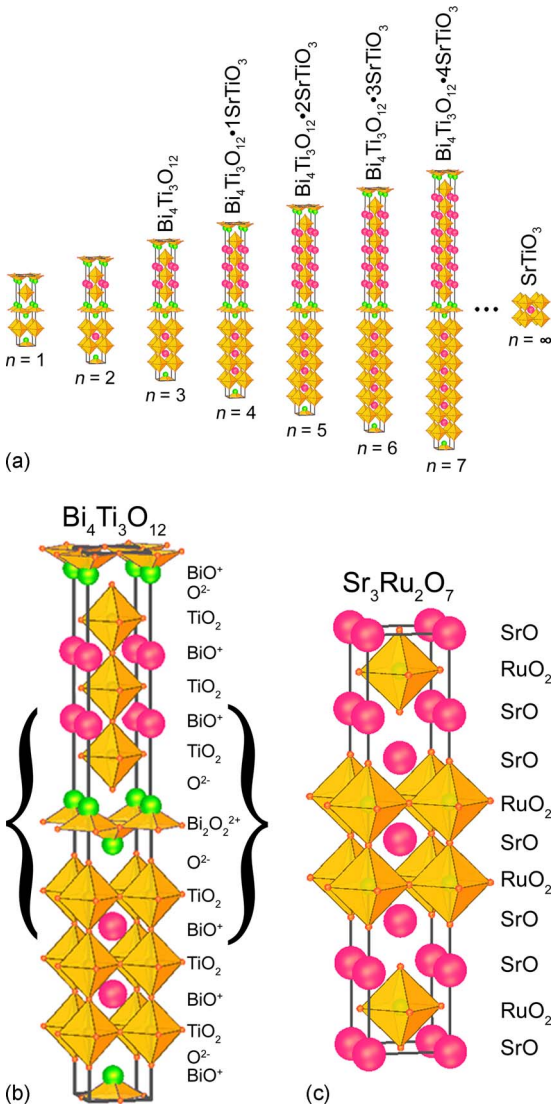

FIG. 1. (Color online) (a) The Aurivillius homologous series of phases, typically written $Bi_2A_{n-1}B_nO_{3n+3}$ but here denoted as $Bi_4Ti_3O_{12}\cdot m SrTiO_3$ where $m=n-3$, consists of alternating $Bi_2O_2^{2+}$ pyramidal layers and n perovskite slab layers. (b) Layer-to-layer charge disparity can stabilize Aurivillius phases in the absence of bulk thermodynamic stability, in contrast to (c) Ruddlesden–Popper phases, with charge-neutral layers. (Charge labels do not imply structural units of crystallization.)

II. CHARGE-MEDIATED SYNTHESIS

$Sr_4Bi_4Ti_7O_{24}$ is an $n=7$ member of the Aurivillius homologous series of layered oxides, which consist of pyramidal $Bi_2O_2^{2+}$ layers alternating with n number of ABO_3 perovskite-type units. The structure at the growth temperature is shown schematically in Fig. 1(a), where n is an integer, A=Sr, Ba, Pb, or Bi, and B is a transition metal, with the chemical formula $Bi_2A_{n-1}B_nO_{3n+3}$. Elastic interactions have been suggested to be responsible for the stabilization of Aurivillius phases,[48] based on the observed basal dimension of square-pyramidal $Bi_2O_2^{2+}$ versus equivalent Bi–O bonding in unconstrained perovskite and bismuth oxide,[49] implying a limit to the spatial extent of this strain interaction. This in turn implies that an Aurivillius phase with sufficiently thick perovskite slabs may exhibit polarization behavior divergent from that of the lower-n members.

Formation of the target phase is encouraged by choosing a stoichiometry which crystallizes in large charge-neutral formula units, adding a strong surface-charge component to the energetics of formation where the free energy of different structures of similar composition is otherwise degenerate. This charge-mediated synthesis requires the selection of constituents having similar coordination chemistry but different charges, leading to minimum charge-neutral crystal units. The example of the $n=3$ Aurivillius phase, $Bi_4Ti_3O_{12}$, is shown in Fig. 1(b), with the composition and formal charge of the individual atomic layers indicated. In this case, both Sr^{2+} and Bi^{3+} can occupy the eight-coordinated A-site of the structure, with Ti^{4+} on the B-sites. This leads to a minimum charge-neutral crystal unit of $Bi_4Ti_2O_{10}$ (indicated by braces) and a single TiO_2 lying between layers. Using this unit as the basis for an Aurivillius subseries with the formula $Bi_4Ti_3O_{12}\cdot m(SrTiO_3)$, where $m=n-3$, it is clear that additional $SrTiO_3$ units can be inserted while maintaining charge neutrality. Charge screening in layered oxides requires several atomic layers;[50] thus a limited number of $SrTiO_3$ units can be inserted into a structure, four in the phase reported here, while still maintaining charge stabilization of the phase of interest. Additionally, as a charge-neutral structural unit forms, the local adatom chemistry modulates strongly, providing further chemical stabilization. A similar mechanism has been described for geologic formation of kaolinite.[51] It should be noted that the approach is not applicable to all layered oxides. For example, every atomic layer of the $Sr_3Ru_2O_7$ shown in Fig. 1(c) is charge neutral, so the minimum unit is a subformula unit, a single atomic layer, thus providing no surface-charge driving force for stabilization of a particular layer order, and indeed most attempts to synthesize higher-n phases consisting of charge-neutral layers suffer intergrowth issues.[10–41]

III. EXPERIMENT

We grew c-axis oriented films of $Sr_4Bi_4Ti_7O_{24}$ on $SrTiO_3$ (001), $LaAlO_3$ $(001)_c$, and $SrRuO_3(001)_c$/$SrTiO_3(001)$ by PLD (Ref. 52) using a KrF excimer laser, $\lambda=248$ nm, from a $Sr_4Bi_{4.6}Ti_7O_{24}$ target, $p_{O_2+O_3}=90$ mTorr, 10 000 pulses, with a substrate temperature of 780–820 °C. Films were quenched immediately after growth in the same atmosphere by dropping them onto the water-cooled walls of the PLD chamber. X-ray diffraction (XRD) characterization was performed using a Picker four-circle x-ray diffractometer using Cu Kα radiation and a graphite monochromator. The chemical composition and structural perfection of the films were investigated by means of Rutherford backscattering (RBS) and channeling using 1.4 MeV He^+ ions. Atomic force microscopy (AFM) imaging was performed in tapping mode. Transmission electron microscopy (TEM) sample preparation was by standard sandwiching and sectioning (for cross sections), and dimple grinding and argon ion milling techniques, using 4.5 kV at 4°–7° for [100] and [110] cross sections and 4.5 kV at 17° incidence and cooling to −180 °C for [001] samples.

In-plane electrical measurements were performed using Au/Cr IDCs on a $Sr_4Bi_4Ti_7O_{24}(001)/LaAlO_3(001)_c$ film 207

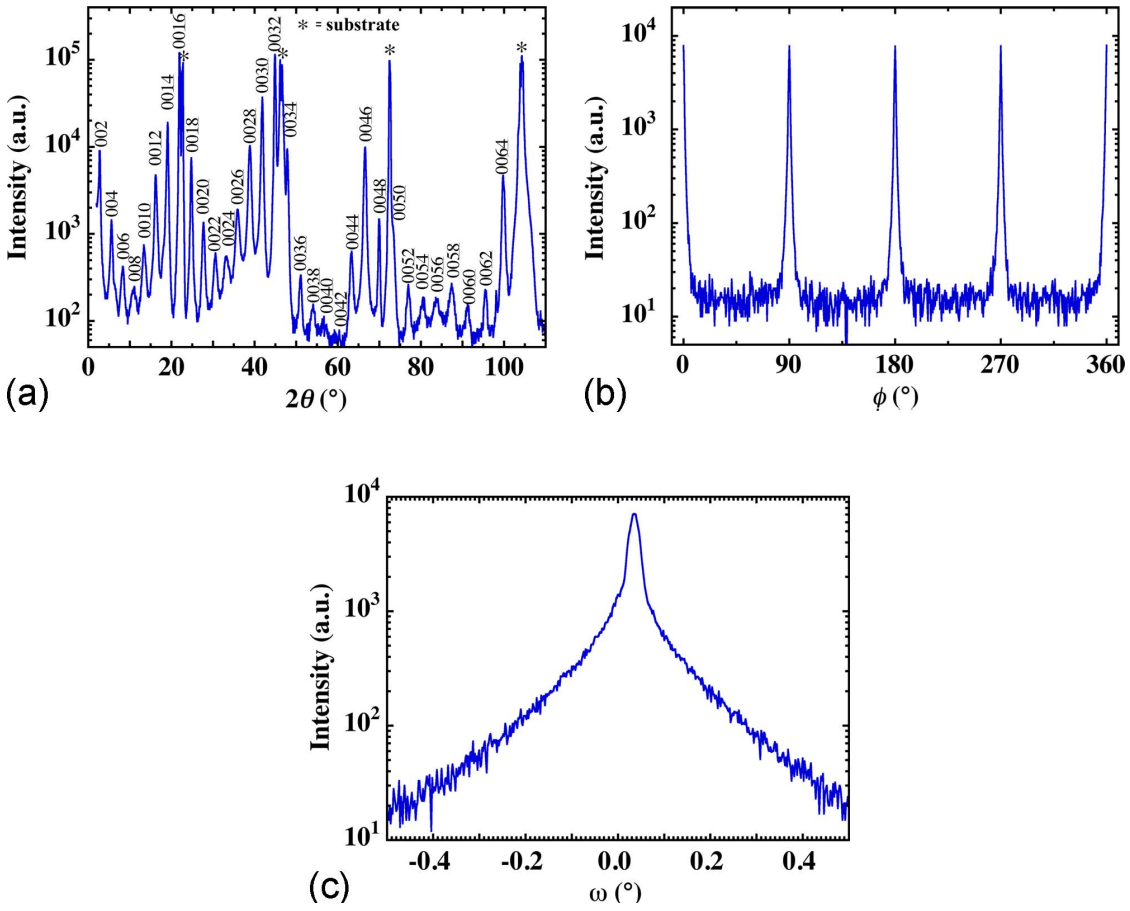

FIG. 2. (Color online) XRD analysis indicates a phase-pure epitaxial $Sr_4Bi_4Ti_7O_{24}$ film. (a) θ-2θ scans indicate a 6.44 nm c-axis lattice parameter, and (b) a ϕ-scan of the 10$\underline{13}$ peak and (c) an ω-scan (rocking curve) of the 00$\underline{32}$ peak indicate high crystalline quality, with FWHMs of 1.0° and 0.03°, respectively.

nm thick, as measured by TEM examination of a nearby region, with devices carefully chosen to lie in regions free of significant thickness gradients, as evidenced by nonvarying optical interference fringes. Measurements were made on IDCs with the in-plane field orientation aligned to the ⟨100⟩, ⟨110⟩, and ⟨120⟩ orthorhombic axes of $Sr_4Bi_4Ti_7O_{24}$. Surface-normal measurements were performed using circular platinum pads on a 225 nm film on a bottom electrode, $SrRuO_3(001)_c/SrTiO_3(001)$, and measured directly under the electrode by sectioning after characterization. The two $Sr_4Bi_4Ti_7O_{24}$ films used for electrical measurements, one with and one without a bottom electrode, were deposited under nearly identical conditions to minimize rocking curve widths, and are considered otherwise identical. Indices are based on an orthorhombic cell with dimensions $a \approx b \approx 0.55$ nm and $c=6.44$ nm, and do not imply the existence or a particular degree of 90° domain switching.

Electronic characterization was performed using computer-controlled impedance analysis and pulse processor data acquisition systems with a Joule–Thompson cooling stage. Samples were poled at ~315 kV/cm for 3 min at 100 K prior to ferroelectric polarization versus temperature measurements. Through-thickness electrical capacitance data were scaled by calibrated optical measurement of the pad size. Remanent polarization was determined based on charge retention in pulse processor measurements and the effective area of the IDC calculated from the definition of capacitance, using an ε_r versus C relation generated from the analytical solution of the IDC data (Sec. IV C). In-plane Q versus E plots are the average of 30 data collections each, to compensate for noise intrinsic to the high-voltage measurement setup.

IV. RESULTS AND DISCUSSION

A. Microstructural characterization

XRD measurements of the samples prepared for this work are in agreement with an $n=7$ Aurivillius phase. The θ-2θ scan of a $Sr_4Bi_4Ti_7O_{24}(001)/SrTiO_3(001)$ film is shown in Fig. 2(a), with $c=6.44$ nm. High crystallinity is implied by peak sharpness, the absence of peak splitting,[53] and the absence of diminished peak heights at low 2θ. Films are epitaxial with minimal texturing, shown in Fig. 2(b) by the 10$\underline{13}$ ϕ-scan (FWHM=1.0°), FWHM (full width at half-maximum) and in Fig. 2(c) by the 00$\underline{32}$ rocking curve (FWHM=0.03°) of the same film. The orientation relationship is $Sr_4Bi_4Ti_7O_{24}(001)\|SrTiO_3(001)$ and $Sr_4Bi_4Ti_7O_{24}[100]\|SrTiO_3[110]$. Films on other substrates exhibit similar crystallinity and orientation. RBS analysis of a sister film grown on $SrTiO_3$ (001), Fig. 3, shows it to be stoichiometric to $Sr_4Bi_4Ti_7O_{24}$ within the experimental error, and minimum RBS channeling yields of $\chi_{min,Bi}=8\%$ and $\chi_{min,Sr}=4\%$ for the bismuth and strontium peaks.

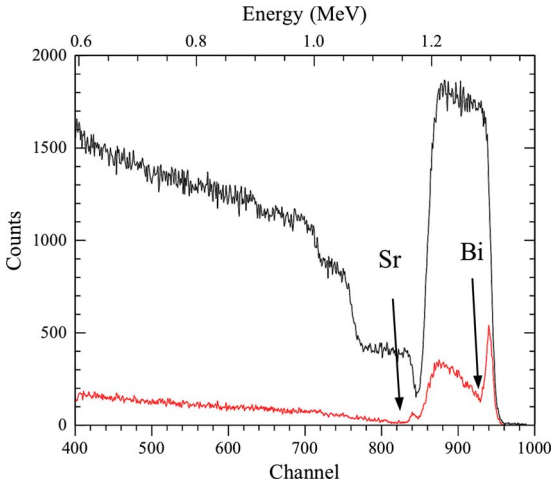

FIG. 3. (Color online) RBS analysis of a sister $Sr_4Bi_4Ti_7O_{24}$ film deposited under identical conditions on a $SrTiO_3$ (001) substrate, showing a stoichiometric composition and high film quality, with $\chi_{min,Bi}=8\%$ and $\chi_{min,Sr}=4\%$.

XRD identification based on θ-2θ 00ℓ reflection positions alone is insufficient to support claims of growth due to the technique's insensitivity to local disorder, although an absence of low-order 00ℓ reflections can be an indication of intergrowths, for example, as seen in randomly intergrown $Bi_4Ti_3O_{12}$–$BaBi_4Ti_4O_{15}$ ($n=3$ and 4) crystals.[54] Furthermore, inclined planar defects of sufficient density may shift the apparent fundamental period of a superlattice when probed by bulk methods such as XRD.[53] Structural sampling at the atomic scale is necessary for conclusive phase identification, such as by high-resolution transmission electron microscopy (HRTEM). The highest-n Aurivillius phase previously reported and confirmed is the $n=6$ material $Bi_7Ti_3Fe_3O_{21}$.[55] All preparations following the stoichiometry of higher-n Aurivillius phases have been shown to consist of intergrowths of two or more n members of the series upon examination by TEM, frequently as semiordered syntactic intergrowths of $n/2$ and $n/2-1$ members.[48] No $n>6$ Aurivillius phase has ever been confirmed.

Mixed-n Aurivillius phases[56,57] can also masquerade in XRD scans as higher-n phases, due to an algebraic artifact of the Aurivillius series of phases. Regions consisting of alternating mixed-n half-cells give rise to peaks in θ-2θ XRD scans that can be inadvertently attributed to a higher-n member with a similar lattice parameter. The dimensions of ABO_3 perovskite layers (denoted as c_P) and of $Bi_2O_2^{2+}$ layers (denoted as c_B) are ~0.4 and ~0.45 nm, respectively, so the long cell dimension c of a given-n Aurivillius phase can be approximated by $c_n=2nc_P+2c_B$. The misidentification risk is therefore clear, as $c_n \approx c_{n/2}+c_{(n/2)-1}$ for even n and similarly as $c_n \approx c_{((n+1)/2)}+c_{((n-3)/2)}$ for odd-n.

Proper identification is further complicated by minor variations in c with variations in synthesis conditions and defect structure. For example, x-ray data indicating a c of ~7.4 nm is sometimes attributed to $n=8$ ($c_{8,theor} \approx 7.3$ nm),[58] but every case that has been submitted to HRTEM examination has revealed the material to be an intergrowth,[14] frequently of $n=3$ and 4 ($c_3+c_4 \approx 7.4$ nm), sometimes ordered over distances of 100 nm or more.[16,17] Similar cases for $n=6$ and 10 exist.[59,60] These syntactic intergrowths exhibit qualitatively different crystallographic symmetry from that of the pure-n phases[61] and have different distributions of atomic site types leading to significantly different electronic behaviors, so it is critical for fundamental studies to distinguish which phase is present. High densities of out-of-phase boundaries (OPBs) can also confound proper indexing in layered phases with large repeat distances.[53]

Cross-section HRTEM examination of a film grown on $LaAlO_3$ $(001)_c$, Fig. 4(a), indicates a 6.4 nm unit cell, corroborating the successful synthesis of an $n=7$ Aurivillius phase, $Sr_4Bi_4Ti_7O_{24}$. A HRTEM phase-contrast image of a single unit-cell thickness is shown in Fig. 4(b), along with a schematic of the structure. Electron diffraction analysis along the [100], [110], and [001] zone axes of a sister film grown on $SrTiO_3$ (001), shown in Fig. 4(c), further confirm a single-phase film of $Sr_4Bi_4Ti_7O_{24}$. Although an orthorhombic $B2cb$ (or monoclinic Pc) symmetry is expected,[62] the observed material appears to be tetragonal, with no discernible distortion at room temperature. This difference is explained by the temperature-dependent electrical measurements, described in Sec. IV B.

The cross-section TEM image of the full film thickness in Fig. 4(d) shows a relatively low density of OPBs (~34/μm in the plane of the film) common in Aurivillius films,[14,53] extending through the film thickness. Features that appear to be bending of $Bi_2O_2^{2+}$ layers are visible, but closer examination reveals them to be closely associated stairlike series of OPBs across which the perovskite slabs are coherent, but with $Bi_2O_2^{2+}$ layers successively sheared along c by a single perovskite subunit at each OPB.[53] These stair-step features have been reported previously in the $n=5$ Aurivillius phase $Ba_2Bi_4Ti_5O_{18}$, in both bulk[14] and thin film[63] forms, and in the $n=6$ $Sr_3Bi_4Ti_6O_{21}$.[64] Their atomic structure has been predicted to consist of the insertion of either an extra perovskite subunit[14] or an extra $Bi_2O_2^{2+}$ double layer.[63] Taking charge balance into consideration, we propose that consecutive $Bi_2O_2^{2+}$ layers would be energetically unfavorable in comparison to the local insertion of an extra perovskite subunit on either side of the step, perhaps composed of $SrTiO_3$, with a 0 charge and negligible contribution to nonstoichiometry. Ordered arrays of such defects are the basis for the related "collapsed" structures,[65] many derived from the Aurivillius prototype. Steps in the film surface ~1/2 unit cell in height (~3.2 nm) are visible in Fig. 4(d), and by AFM, shown in Fig. 5, which also reveals growth spirals emanating from screw dislocations (or dislocations with a screw component)[66,67] with an apparent Burgers vector of $\mathbf{b} \approx 6.4$ nm.

B. Electrical behavior

Permittivity (ε) versus temperature behavior of $Sr_4Bi_4Ti_7O_{24}$ along the ⟨100⟩, ⟨110⟩, and ⟨001⟩ (orthorhombic axes) of the ferroelectric phase are shown in Fig. 6(a), measured on the same film used for the TEM imaging in Sec. IV A, and on the sister film grown on a $SrRuO_3$ bottom electrode. Indices are based on an orthorhombic cell, and do not imply the existence or a particular degree of 90° domain

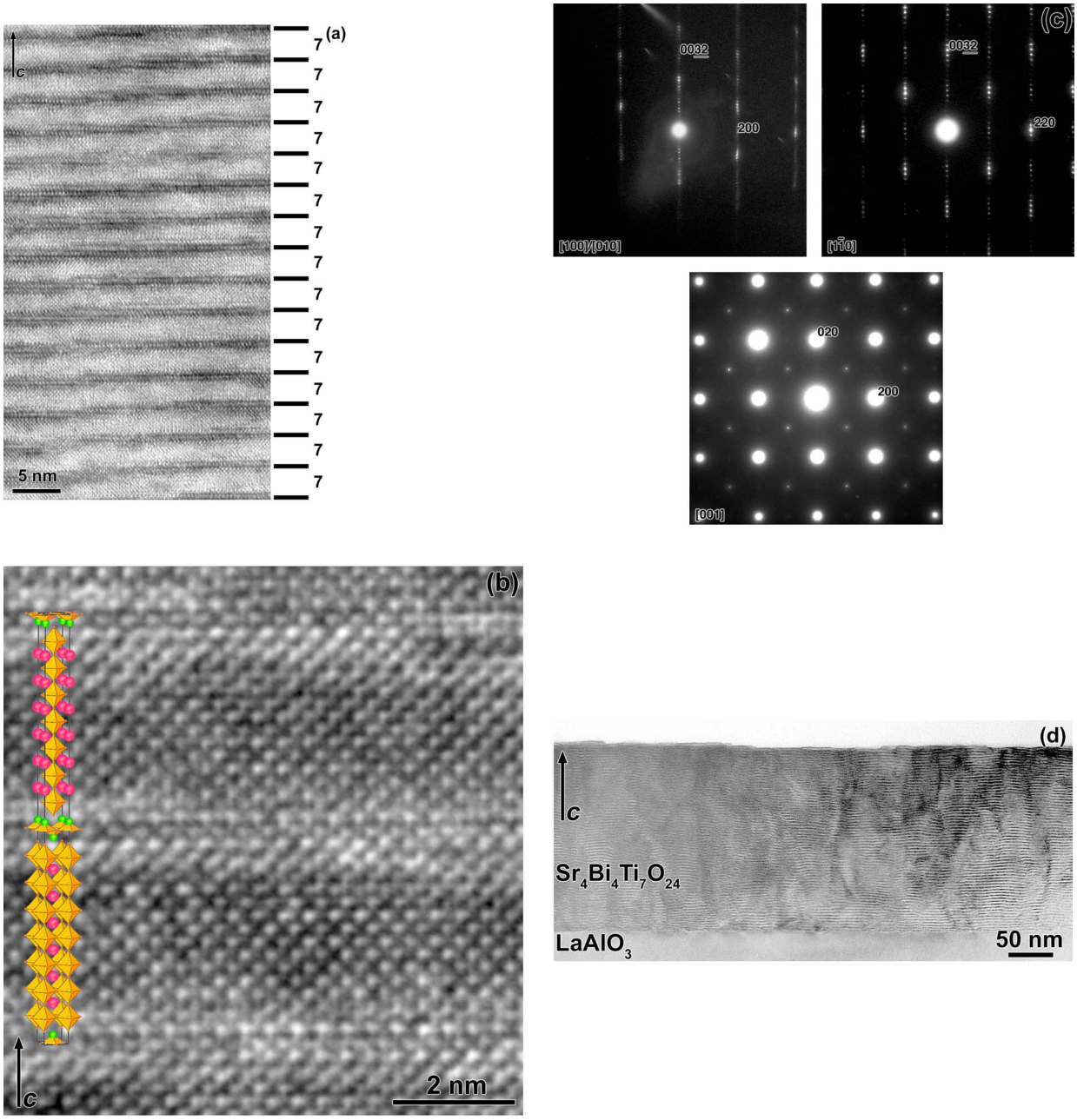

FIG. 4. (Color online) TEM analysis confirms the successful synthesis of phase-pure $Sr_4Bi_4Ti_7O_{24}$. (a) Cross-section HRTEM image demonstrating a single-phase $Sr_4Bi_4Ti_7O_{24}$ film. The horizontal dark bands of contrast correspond to the $Bi_2O_2^{2+}$ layers. (b) HRTEM image of a single unit cell and corresponding schematic of the crystal structure. (c) Electron diffraction patterns taken along the three principal crystal axes. (d) Cross-section TEM of the full film thickness shows regular spacing through the film thickness. A low density of OPB defects, many dissociated over several nanometers in the *ab* plane, is apparent.

switching. The Curie point is 324 K at 10 kHz, which explains the apparent tetragonal symmetry observed by electron diffraction described above, considering that the electron beam heats a specimen by several tens of degrees above room temperature. Relaxorlike dielectric behavior is seen in the plane of the layering, characterized by a broadening of the transition and a frequency dispersion of the dielectric response. Vogel–Fulcher analysis was inconclusive due to the limited frequency range of our equipment setup. Out-of-plane dielectric behavior is linear with a low ε, in the lower region of the plot.

The T_C of $Sr_4Bi_4Ti_7O_{24}$ is on trend with other values reported for this family of $Bi_4Ti_3O_{12}\cdot m(SrTiO_3)$ materials,[68,69] shown in Fig. 6(b). The emergence of relaxorlike behavior may indicate that some $SrTiO_3$ units in the perovskite slab exhibit similar behavior to bulk $SrTiO_3$, indicating that the spatial limits of interlayer interaction in a layered complex oxide may be reached in this phase. Similarly, studies of $Bi_4Ti_3O_{12}\cdot m PbTiO_3$ ($m=0-3$) showed the appearance of clear relaxor behavior in $m=2$ and 3 compositions.[70] Bulk $SrTiO_3$ is an incipient ferroelectric, with an increased dielectric constant, but no ferroelectric transition down to 0 K. Relaxor behavior has not been reported for these $Bi_2O_2(Sr_{n-1}Ti_nO_{3n+1})$ Aurivillius materials, which are reported to exhibit sharp transitions without fre-

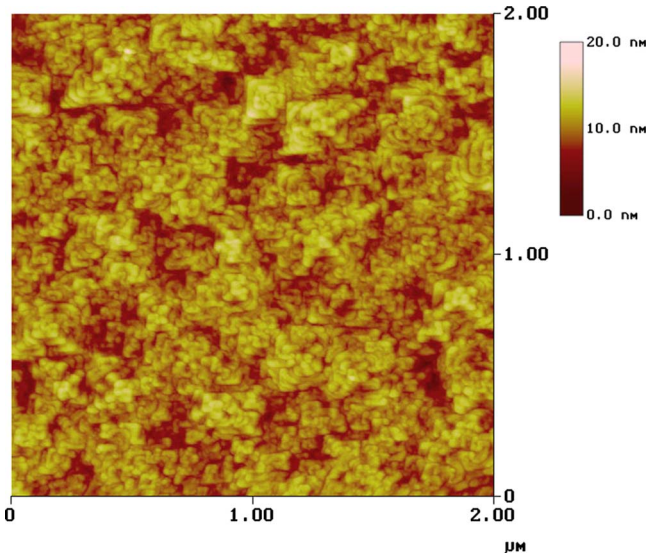

FIG. 5. (Color online) AFM image of the surface of the $Sr_4Bi_4Ti_7O_{24}$ film, showing growth spirals emanating from dislocations with screw component on the surface with formula-unit steps 3.2 nm in height.

quency dispersion, such as the $n=4$ $SrBi_4Ti_4O_{12}$ (Ref. 71) and the $n=6$ $Sr_3Bi_4Ti_6O_{21}$.[72] Double-substituted (simultaneous *A* and *B*) Aurivillius phases also reportedly exhibit relaxor-type behavior, but these are all essentially aliovalently substituted,[70,73,74] or are different phases altogether.[75] In bulk $SrTiO_3$, bismuth or calcium doping is known to induce relaxorlike behavior.[76,77] Although relaxor behavior is reported for lower-*n* members of both Ba- and Pb-based Aurivillius systems,[68] the 2+ valence of these cations versus the 3+ of bismuth may limit the spatial modulation of the ionization state of the other cations, which can itself lead to relaxorlike behavior.

Charge versus electrical field measurements also indicate electrical behavior out of character with other $Bi_2Sr_{n-1}Ti_nO_{3n+3}$ Aurivillius phases. Odd-*n* Aurivillius phases are predicted to exhibit orthorhombic *B*2*cb* (or monoclinic *Pm*) symmetry,[62] and therefore may have a polar axis in the *a*-*c* plane, and thus may have a component of polarization along *c*. But, in this $Sr_4Bi_4Ti_7O_{24}$ film, linear dielectric behavior along *c* is observed. Piezoresponse microscopy measurements up to 440 kV/cm along ⟨001⟩ (not shown), and charge-retention measurements up to 3000 kV/cm along ⟨001⟩, Fig. 7, show no evidence of any ferroelectric remanence along *c*. Any remanence would be entirely in the (001) plane.

The in-plane charge-retention measurements collected along the ⟨100⟩ and ⟨110⟩ axes are also shown in Fig. 7. In-plane remanent polarization is 5.2 $\mu C/cm^2$ along ⟨100⟩, and 4.1 $\mu C/cm^2$ along ⟨110⟩. The inset of Fig. 7 shows the same data, rescaled with the relatively large (linear) dielectric contribution subtracted, to show clearly to the eye that the ferroelectric polarization loops have low loss. Further measurements, such as low-temperature electron diffraction analysis, are expected to clarify issues of symmetry and hence the polar axis. P_r versus *T* measurements which were not possible due to noise of the high fields necessary with our electrode geometry, would also be informative.

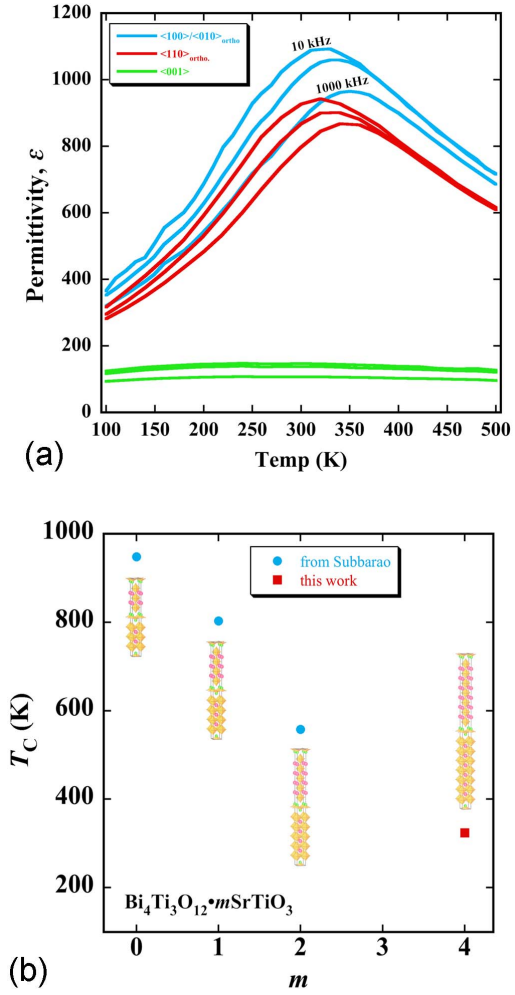

FIG. 6. (Color online) (a) Impedance analysis shows some indications of relaxorlike behavior in-plane (10, 100, and 1000 kHz) and a $T_C=324$ K in this dielectric constant vs temperature plot. (b) T_C vs *m* for $Bi_4Ti_3O_{12}\cdot m(SrTiO_3)$ phases. Prior data are taken from Refs. 68 and 69. Bulk $SrTiO_3$ has no ferroelectric transition down to 0 K.

The axis of polarization was determined to lie 9.7° from ⟨100⟩ about (001) by vector projection analysis of the ε or P_r values measured along the ⟨100⟩, ⟨110⟩, and ⟨120⟩ (not shown) axes. The values for the ε and P_r values of all three orientations differ by $\leq 2.3\%$ from the vector-averaged value. This is in contrast to the case where a ⟨100⟩ axis is assumed, which would result in an $\sim 17\%$ disagreement between ⟨100⟩ and ⟨110⟩ measurements of both ε_r and P_r.

From a symmetry perspective, such a direction for the spontaneous polarization is inconsistent with the expected space group *B*2*cb* (or *Bm*).[62,78] A possible explanation is that 90° domains exist in the $Sr_4Bi_4Ti_7O_{24}$ films and that the applied electric field used in the measurements was sufficient to switch 180° domains but not the 90° domains. As the films are grown at a substrate temperature well above T_C, 90° domains are expected to form on cooling through T_C. Different populations of domains along [100] versus [010] in combination with insufficiently high electric field to switch the 90° domains could lead to what looks like a polarization inclined from the [100] axis.

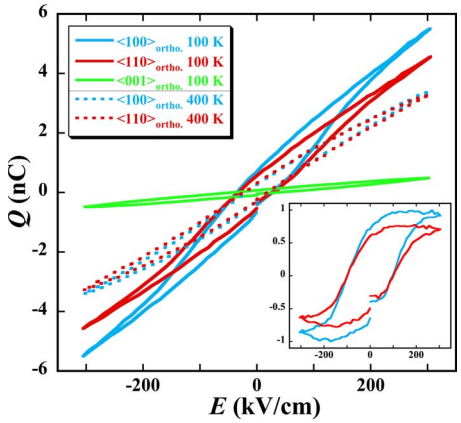

FIG. 7. (Color online) Charge vs electrical field measurements reveal ferroelectric behavior in-plane appreciably below T_C at 100 K (solid lines) and only slight nonlinearity above T_C (dashed lines), which is still in the transition region due to the broadness of the transition. The inset shows the same data scaled to remove the relatively high linear dielectric contribution to show to the eye a ferroelectric polarization loop with low loss.

C. Interpretation of IDC data

Interpretation of IDC capacitance measurements of thin films is complicated by fringing fields and the differential penetration of the electric field through layers of different dielectric constants. The system cannot be described by a simple approximation to a parallel plate capacitor. Reported approaches to deriving permittivity from experimental data were evaluated for applicability to the system under study but were found to be insufficient. A finite-element model of the system was developed and assessed in relation to previous approaches. A schematic of the IDC used in this work is shown in Fig. 8, with the relevant dimensions of finger spacing s, finger width d, and finger length L labeled, and a number of fingers N of 48 and film thickness h. Previous approaches have focused on empirical or analytical solutions to the problem of the capacitance of a periodic two-dimensional electrode pattern on a dielectric slab. The approach of Farnell derives empirical formulas based on a fit of results of numerical simulations of the capacitance of two parallel metallic strips patterned on a two-layer substrate.[79] These results are valid for an IDC on an infinite dielectric slab and therefore not directly applicable to a thin film on a dielectric substrate.

A partial capacitance approach is valid for this structure and was taken by both Gevorgian[80] and Vendik *et al.*,[81] as an approximation enabled by a large difference in dielectric constant between the ferroelectric layer and the dielectric substrate. There are three contributions to the capacitance of the structure; air, film, and substrate. The measured capacitance takes the form

$$C_{\text{measured}} = C_{\text{ad}} + K \cdot (\varepsilon_f - \varepsilon_s), \tag{1}$$

where $\varepsilon_f \gg \varepsilon_s$ are the dielectric constants of the ferroelectric and substrate, respectively, C_{ad} is the contribution of the air and substrate to the total capacitance of the IDC, and K is a proportionality factor with units of picofarad. The formula yields the dielectric constant of the ferroelectric

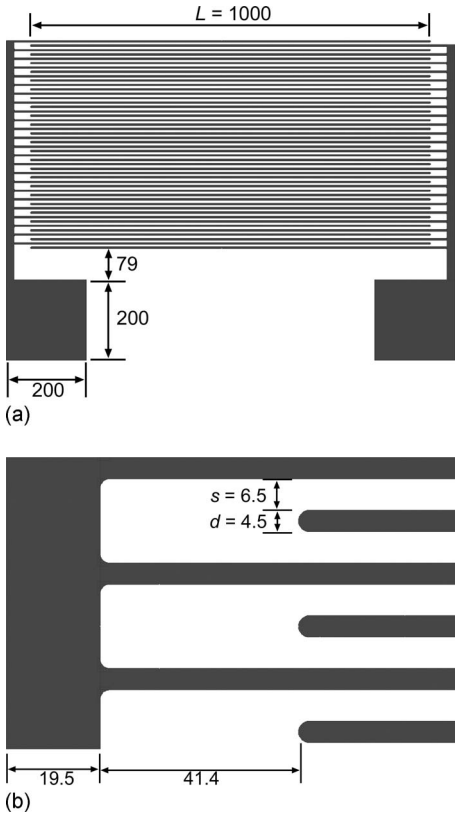

FIG. 8. Schematics of the IDC modeled for this study. (a) Overview and (b) detail, showing variables and dimensions in microns.

$$\varepsilon_f = \varepsilon_s + \frac{C_{\text{measured}}}{K} - \frac{C_{\text{ad}}}{K}. \tag{2}$$

The method of Gevorgian *et al.*[80] employs a conformal mapping technique to calculate an analytical solution to the capacitance of an electrode pattern on a two-layered substrate, with a correction for the finite number of fingers and their finite length. It provides solutions for several cases, but they point out that its validity does not extend to cases for which $h \ll d$ ($t \ll d$ in their notation).[80] The method of Vendik *et al.*[81] also employs a conformal mapping technique to analytically calculate the mutual capacitance of two metallic strips patterned on a two-layered substrate,[81] and is further developed by numerical methods,[82] multiplied by the number of gaps in the IDC, $N_{\text{slots}}=N-1$. This approach may be inaccurate as it does not explicitly take into account the periodicity of the electrode pattern. It is unclear why the approach yields the results divergent from our and the other approaches, although it is clearly not due to the finite number of fingers or their finite length, which, for our electrode configuration, influence the capacitance on the level of 0.1 pF. The calculated values for C_{ad} are also summarized in Table I.

Results for K obtained using Refs. 80 and 81 are essentially identical. The result obtained according to Ref. 79 differs by ~10%. We believe that this latter result is less accurate because small h/s was not especially considered, and in our case this ratio is about 0.02.

We have treated this problem with a finite-element model developed in FEMLAB/MATLAB using the partial capacitance approach to analyze the capacitance data of the

TABLE I. Results of calculation of the proportionality factor and the contributions by air and the substrate to the total capacitance measured on the IDC on the $Sr_4Bi_4Ti_7O_{24}$ films, shown for both reported approaches and for this work.

Calculated Value	Ref. 80	Ref. 81	Ref. 82	This work
K (pF)	0.00897	0.00898	···	···
C_{ad} (pF)	4.35	6.3	4.8	4.7
C_{film} for ε_f=1000, (pF)	8.75	8.76	···	···

experiment to determine the dielectric permittivity of the film. The ε of the $LaAlO_3$ substrate varies by $<1\%$ over the temperature range of interest.[83] We use a value of $K=(9\pm0.5)\times10^{-3}$ for the considered electrode structure, with an accuracy about 5%, and $C_{ad}=4.8\pm0.1$ pF as the average of the results obtained with numerical analyses of the periodic domain pattern. Thus, ε_f can be calculated from Eq. (1). The inaccuracy in the additional capacitance $\Delta C_{ad}=0.1$ pF leads to an inaccuracy of the calculated value of the permittivity of the ferroelectric $\Delta\varepsilon_f=\Delta C_{ad}/K\approx10$. Note that this is a systematic error in the absolute value of ε_f, which does not affect the shape of the curve $\varepsilon_f(T)$ and the position of its maximum. The accuracy of the calculation of ε_f is 5%.

Figure 9(a) shows a comparison of the results of the different models as applied to our IDC, with results for ε_f differing by ~13%. The results of our calculations can also be used for conversion of measured capacitance to dielectric constant for films of similar thickness on the same substrate, $LaAlO_3$, with a conversion of $\varepsilon=72464$, $C-291.22$. This is considered valid for identical test structures on films of similar thickness (210 nm) but presumably can be scaled by the thickness function F described in a numerical study of IDC.[84] The relation is also considered valid for films having capacitance in the range from 2 to 20 pF. Efforts to expand the method to include other substrate materials are underway.

V. CONCLUSIONS

Charge-mediated synthesis was used to formulate a high-n Aurivillius phase, synthesized by PLD, and confirmed by diffraction and microscopic analysis, including phase-pure synthesis of an Aurivillius phase with the largest lattice period ever reported. It is hypothesized that epitaxial constraint, which stabilizes the (001) orientation, further contributes to the stabilization by forcing non-charge-neutral layers to form in sequence along c (perpendicular to the $Bi_2O_2^{2+}$ sheets). $Sr_4Bi_4Ti_7O_{24}$ exhibits electronic behaviors divergent from other members of the same composition series: indications of relaxorlike behavior, an apparent lack of a component of polarization along c, and a potentially different symmetry. It is anticipated that successful synthesis of subsequent series members will yield further insight into the spatial extent of interlayer interactions in layered perovskite complex oxides.

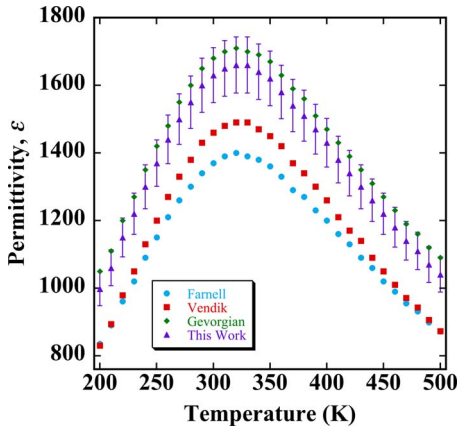

FIG. 9. (Color online) Comparison of the application of the different models for the extraction of permittivity from capacitance data collected at 10 kHz.

ACKNOWLEDGMENTS

This work was supported by The Aerospace Corporation's Independent Research and Development Program. The authors also gratefully acknowledge the financial support of the National Science Foundation through Grant Nos. DMR-0507146 and DMR-0820404 and the U.S. Department of Energy through Contract No. W-31-109-ENG-38. Work at Argonne National Laboratory, and use of Argonne's Center for Nanoscale Materials and Electron Microscopy Center was supported by the U.S. Department of Energy, Office of Science, Office of Basic Energy Sciences, under Contract No. DE-AC02-06CH11357. The authors thank Professor Susan Trolier-McKinstry for helpful discussions.

[1] Y. Moritomo, A. Asamitsu, H. Kuwahara, and Y. Tokura, Nature (London) **380**, 141 (1996).
[2] C. A. Paz de Araujo, J. D. Cuchiaro, L. D. McMillan, M. C. Scott, and J. F. Scott, Nature (London) **374**, 627 (1995).
[3] M. A. Zurbuchen, R. S. Freitas, M. J. Wilson, P. Schiffer, M. Roeckerath, J. Schubert, G. H. Mehta, D. J. Comstock, J. H. Lee, Y. Jia, and D. G. Schlom, Appl. Phys. Lett. **91**, 033113 (2007).
[4] K. Koumoto, I. Terasaki, and R. Funahashi, MRS Bull. **31**, 206 (2006).
[5] J. G. Bednorz, K. A. Muller, and M. Takashige, Science **236**, 73 (1987).
[6] M. A. Zurbuchen, G. Asayama, D. G. Schlom, and S. K. Streiffer, Phys. Rev. Lett. **88**, 107601 (2002).
[7] M. Imada, A. Fujimori, and Y. Tokura, Rev. Mod. Phys. **70**, 1039 (1998).
[8] J. S. Anderson, in *The Chemistry of Extended Defects in Non-Metallic Solids: Proceedings of the Institute for Advanced Study on the Chemistry of Extended Defects in Non-Metallic Solids*, edited by L. Eyring and M. O'Keefe (North-Holland, Scottsdale, AZ, 1969) pp. 1–20.
[9] K. R. Udayakumar and A. N. Cormack, J. Am. Ceram. Soc. **71**, C469 (1988).
[10] B. G. Hyde and S. Andersson, *Inorganic Crystal Structures* (Wiley-Interscience, New York, 1989).
[11] C. N. R. Rao and B. Raveau, *Transition Metal Oxides: Structure, Properties, and Synthesis of Ceramic Oxides*, 2nd ed. (Wiley-VCH, New York, 1998), pp. 61–226.
[12] D. R. Veblen, Am. Mineral. **76**, 801 (1991).
[13] R. J. D. Tilley, J. Solid State Chem. **21**, 293 (1977).
[14] J. L. Hutchison, J. S. Anderson, and C. N. R. Rao, Proc. R. Soc. London, Ser. A **355**, 301 (1977).
[15] J. Drennan, C. P. Tavares, and B. C. H. Steele, Mater. Res. Bull. **17**, 621 (1982).
[16] J. Gopalakrishnan, A. Ramanan, C. N. R. Rao, D. A. Jefferson, and D. J. Smith, J. Solid State Chem. **55**, 101 (1984).
[17] D. A. Jefferson, M. K. Uppal, C. N. R. Rao, and D. J. Smith, Mater. Res. Bull. **19**, 1403 (1984).
[18] C. N. R. Rao and J. M. Thomas, Acc. Chem. Res. **18**, 113 (1985).
[19] R. A. Mohan Ram, L. Ganapathi, P. Ganguly, and C. N. R. Rao, J. Solid State Chem. **63**, 139 (1986).
[20] J. M. Tarascon, W. R. McKinnon, P. Barboux, D. M. Hwang, B. G. Bagley, L. H. Greene, G. W. Hull, Y. LePage, N. Stoffel, and M. Giroud, Phys. Rev. B **38**, 8885 (1988).
[21] B. Raveau, C. Michel, and M. Hervieu, in *Advances in Superconductivity:*

Proceedings of the 1st International Symposium on Superconductivity (ISS '88), edited by K. Kitazawa and T. Ishiguro (Springer-Verlag, Tokyo, 1989), pp. 151–157.
[22]W. T. Fu, H. W. Zandbergen, Q. Xu, J. M. van Ruitenbeek, L. J. de Jongh, and G. van Tendeloo, Solid State Commun. **70**, 1117 (1989).
[23]O. Eibl, Physica C **168**, 249 (1990).
[24]R. Ramesh, S. Jin, and P. Marsh, Nature (London) **346**, 420 (1990).
[25]A. Nozaki, H. Yoshikawa, T. Wada, H. Yamauchi, and S. Tanaka, Phys. Rev. B **43**, 181 (1991).
[26]M. A. Señaris-Rodriguez, A. M. Chippindale, A. Várez, E. Morán, and M. A. Alario-Franco, Physica C **172**, 477 (1991).
[27]R. J. Cava, T. Siegrist, B. Hessen, J. J. Krajewski, W. F. Peck, Jr., B. Batlogg, H. Takagi, J. V. Waszczak, L. F. Schneemeyer, and H. W. Zandbergen, J. Solid State Chem. **94**, 170 (1991).
[28]K. Hawkins and T. J. White, Philos. Trans. R. Soc. London, Ser. A **336**, 541 (1991).
[29]T. Williams, F. Lichtenberg, A. Reller, and G. Bednorz, Mater. Res. Bull. **26**, 763 (1991).
[30]A. Schilling, M. Cantoni, J. D. Guo, and H. R. Ott, Nature (London) **363**, 56 (1993).
[31]M. Čeh, V. Kraševec, and D. Kolar, J. Solid State Chem. **103**, 263 (1993).
[32]S. Adachi, H. Yamauchi, S. Tanaka, and N. Môri, Physica C **212**, 164 (1993).
[33]Z. Hiroi, M. Takano, M. Azuma, and Y. Takeda, Nature (London) **364**, 315 (1993).
[34]X.-J. Wu, S. Adachi, C.-Q. Jin, H. Yamauchi, and S. Tanaka, Physica C **223**, 243 (1994).
[35]P. Laffez, G. Van Tendeloo, R. Seshadri, M. Hervieu, C. Martin, A. Maignan, and B. Raveau, J. Appl. Phys. **80**, 5850 (1996).
[36]M. A. McCoy, R. W. Grimes, and W. E. Lee, Philos. Mag. A **75**, 833 (1997).
[37]R. Seshadri, M. Hervieu, C. Martin, A. Maignan, B. Domenges, B. Raveau, and A. N. Fitch, Chem. Mater. **9**, 1778 (1997).
[38]S. D. Bader, R. M. Osgood III, D. J. Miller, J. F. Mitchell, and J. S. Jiang, J. Appl. Phys. **83**, 6385 (1998).
[39]J. Sloan, P. D. Battle, M. A. Green, M. J. Rosseinsky, and J. F. Vente, J. Solid State Chem. **138**, 135 (1998).
[40]K. Szot and W. Speier, Phys. Rev. B **60**, 5909 (1999).
[41]G. Trolliard, N. Ténèze, P. Boullay, and D. Mercurio, J. Solid State Chem. **177**, 1188 (2004).
[42]W. Tian, X. Q. Pan, J. H. Haeni, and D. G. Schlom, J. Mater. Res. **16**, 2013 (2001).
[43]C. D. Theis, J. Yeh, D. G. Schlom, M. E. Hawley, G. W. Brown, J. C. Jiang, and X. Q. Pan, Appl. Phys. Lett. **72**, 2817 (1998).
[44]I. Bozovic and J. N. Eckstein, in *Physics of High-Temperature Superconductors*, edited by D. Ginsberg (World Scientific, River Edge, NJ, 1996), Vol. 5.
[45]J. H. Haeni, C. D. Theis, D. G. Schlom, W. Tian, X. Q. Pan, H. Chang, I. Takeuch, and X. D. Xiang, Appl. Phys. Lett. **78**, 3292 (2001).
[46]B. Mercey, P. A. Salvador, W. Prellier, T.-D. Doan, J. Wolfman, J.-F. Hamet, M. Hervieu, and B. Raveau, J. Mater. Chem. **9**, 233 (1999).
[47]D. P. Norton, B. C. Chakoumakos, D. H. Lowndes, and J. D. Budai, Appl. Surf. Sci. **96–98**, 672 (1996).
[48]B. Frit and J. P. Mercurio, J. Alloys Compd. **188**, 27 (1992).
[49]R. A. Armstrong and R. E. Newnham, Mater. Res. Bull. **7**, 1025 (1972).
[50]A. Ohtomo, D. A. Muller, J. L. Grazul, and H. Y. Hwang, Nature (London) **419**, 378 (2002).
[51]S. B. Hendricks, Am. Mineral. **40**, 139 (1955).
[52]The subscript c indicates pseudocubic cell.
[53]M. A. Zurbuchen, W. Tian, X. Q. Pan, D. Fong, S. K. Streiffer, M. E. Hawley, J. Lettieri, Y. Jia, G. Asayama, S. J. Fulk, D. J. Comstock, S. Knapp, A. H. Carim, and D. G. Schlom, J. Mater. Res. **22**, 1439 (2007).
[54]T. Kobayashi, Y. Noguchi, and M. Miyayama, Appl. Phys. Lett. **86**, 012907 (2005).
[55]G. N. Subbanna, L. Ganapathi, and C. N. R. Rao, Mater. Res. Bull. **22**, 205 (1987).
[56]T. Kikuchi, J. Less-Common Met. **52**, 163 (1977).
[57]T. Kikuchi, J. Less-Common Met. **48**, 319 (1976).
[58]I. G. Ismailzade, V. I. Nesterenko, F. A. Mirishli, and P. G. Rustamov, Kristallografiya **12**, 400 (1967).
[59]S. Horiuchi, T. Kikuchi, and M. Goto, Acta Crystallogr., Sect. A: Cryst. Phys., Diffr., Theor. Gen. Crystallogr. **33**, 701 (1977).
[60]K. Muramatsu, M. Shimazu, J. Tanaka, and S. Horiuchi, J. Solid State Chem. **36**, 179 (1981).
[61]P. Boullay and D. Mercurio, Integr. Ferroelectr. **62**, 149 (2004).
[62]R. E. Newnham, R. W. Wolfe, and J. F. Dorrian, Mater. Res. Bull. **6**, 1029 (1971).
[63]D. Hesse, N. D. Zakharov, A. Pignolet, A. R. James, and S. Senz, Cryst. Res. Technol. **35**, 641 (2000).
[64]S. T. Zhang, Y. F. Chen, H. P. Sun, X. Q. Pan, W. S. Tan, Z. G. Liu, and N. B. Ming, J. Appl. Phys. **94**, 544 (2003).
[65]O. Pérez, H. Leligny, G. Baldnozzi, D. Grebille, M. Hervieu, P. Labbé, D. Groult, and H. Graafsma, Phys. Rev. B **56**, 5662 (1997).
[66]F. C. Frank, Discuss. Faraday Soc **5**, 48 (1949).
[67]W.K. Burton, N. Cabrera, and F. C. Frank, Philos. Trans. R. Soc. London, Ser. A **243**, 299 (1951); F. C. Frank, Adv. Phys. **1**, 91 (1952).
[68]E. C. Subbarao, J. Phys. Chem. Solids **23**, 665 (1962).
[69]E. C. Subbarao, Phys. Rev. **122**, 804 (1961).
[70]J. F. Fernández, A. C. Caballero, M. Villegas, J. de Frutos, and L. Lascano, Appl. Phys. Lett. **81**, 4811 (2002).
[71]Y. Noguchi, M. Miyayama, and T. Kudo, Appl. Phys. Lett. **77**, 3639 (2000).
[72]S. T. Zhang, Y. F. Chen, H. P. Sun, X. Q. Pan, W. S. Tan, Z. G. Liu, and N. B. Ming, J. Phys.: Condens. Matter **15**, 1223 (2003).
[73]D. B. Jennet, P. Marchet, M. El Maaoui, and J. P. Mercurio, Mater. Lett. **59**, 376 (2005).
[74]J. Tellier, P. Boullay, D. B. Jennet, and D. Mercurio, Solid State Sci. **10**, 177 (2008).
[75]G. I. Skavani, Ia. M. Ksendzov, V. A. Trigubenko, and V. G. Prokhvatilov, Sov. Phys. JETP **6**, 250 (1958).
[76]G. A. Smolenskii, V. A. Isupov, A. I. Agranovskaya, and S. N. Popov, Sov. Phys.: Solid State **2**, 2584 (1967).
[77]J. G. Bednorz and K. A. Muller, Phys. Rev. Lett. **52**, 2289 (1984).
[78]R. E. Newnham, *Properties of Materials: Anisotropy, Symmetry, Structure* (Oxford, New York, 2005).
[79]G. W. Farnell, I. A. Cermak, P. Silvester, and S. K. Wong, IEEE Trans. Sonics Ultrason. **17**, 188 (1970).
[80]S. S. Gevorgian, T. Martinsson, P. L. Linner, and E. L. Kollberg, IEEE Trans. Microwave Theory Tech. **44**, 896 (1996).
[81]O. G. Vendik, S. P. Zubko, and M. A. Nikolskii, Tech. Phys. **44**, 349 (1999).
[82]I. Vendik, O. G. Vendik, A. N. Deleniv, V. V. Kondratiev, M. N. Goubina, and D. V. Kholodniak, IEEE Trans. Microwave Theory Tech. **48**, 1247 (2000).
[83]J. Krupka, R. G. Geyer, M. Kuhn, and J. H. Hinken, IEEE Trans. Microwave Theory Tech. **42**, 1886 (1994).
[84]N. J. Kidner, Z. J. Homrighaus, T. O. Mason, and E. J. Garboczi, Thin Solid Films **496**, 539 (2006).